Electronic Supplementary Material (ESI) for Journal of Materials Chemistry C.

Supplementary Information

A General Approach for All-visible-light Switching of Diarylethenes through Triplet Sensitization using Semiconducting Nanocrystals

Lili Hou,[a,b,c] Wera Larsson,[a] Stefan Hecht,[d,e] Joakim Andréasson,[a] Bo Albinsson,*[a]*

[a] Department of Chemistry and Chemical Engineering, Chalmers University of Technology, Gothenburg 412 96, Sweden.

[b] Present Address: School of Precision Instruments and Optoelectronics Engineering, Tianjin University, Tianjin 300072, China.

[c] Present Address: Key Laboratory of Optoelectronics Information Technology, Ministry of Education, Tianjin 300072, China.

[d] Department of Chemistry & IRIS Adlershof, Humboldt-Universität zu Berlin, Brook-Taylor-Str. 2, 12489 Berlin, Germany.

[e] DWI—Leibniz Institute for Interactive Materials & Institute of Technical and Macromolecular Chemistry at RWTH Aachen University, 52074 Aachen, Germany.

*Corresponding author e-mails: lilihou@tju.edu.cn; balb@chalmers.se

Contents

1. Methods and Experiments

Chemicals

Analytical reagent grade toluene from VWR was used without further purification for spectroscopic measurements. 1,2-bis(2,4-dimethyl-5-phenyl-3-thienyl)-3,3,4,4,5,5-hexafluoro-1-cyclopentene (DAE2) and 1-pyrenecarboxylic acid (PyCOOH) were purchased from TCI. Phenanthrene was purchased from Fluka A.G. The detailed synthesis of 3-PCA, DAE1, DAE3 and DAE4 was according to previous reports.[1-4] CdS NCs were prepared by a slightly modified synthesis according to previous reports.[5, 6]

Cadmium oxide, sulfur powder, 1-octadecene, and dioxane were purchased from Sigma Aldrich. Oleic acid was purchased from Alfa Aesar. 3-acetylphenanthrene was purchased from Acros Organics, sodium hypochlorite solution was purchased from Scharlau Chemie, and diethyl ether was purchased from Fisher Chemicals. All the chemicals were used without further purification steps.

Synthesis

257 mg of CdO, 6 ml of oleic acid and 15.8 ml of ODE were mixed in a 50 ml three-necked flask, which was degassed under vacuum at 110 °C for 1 hour. After that, the solution was heated to 260 °C under N_2 until the mixture turned colorless and clear. 32 mg of sulfur was dissolved in 3 ml of ODE, and degassed under N_2 for 30 minutes, followed by sonication for at least 1 hour. The sulfur solution was injected into the Cd solution at 210 °C. After injection, the solutions were cooled by compressed air to 150-190 °C according to the size required. UV-visible absorption spectra of the aliquots were measured during the reaction. Once the first absorption peak of the CdS NCs reached the desired wavelength, the reaction was stopped by fast cooling to room temperature. The obtained CdS NCs were further purified by extraction with hexane/acetonitrile three times and precipitated with acetone twice.

Spectroscopies

UV-visible absorption spectra were measured using a Cary 50 UV-vis-NIR spectrophotometer. Steady-state fluorescence spectra were recorded on a Cary Eclipse fluorescence spectrophotometer. Fluorescence lifetime measurements were carried out using time-correlated single photon counting (TCSPC), which was excited by a 405 nm laser diode (PicoQuant) and recorded by an MCP-PMT detector (10 000 counts, 2048 channels). Time-resolved transient absorption measurements were carried out on a home-built system, in which an Nd:YAG laser (10 ns, 10 Hz, Spectra-Physics, Quanta-Ray) equipped with an OPO (Spectra-Physics, primoScan) was used as a pump beam, and a quartz-halogen lamp was used as a probe light. The time-resolved decays were measured on a 9 stage PMT (Applied Photophysics) coupled with a monochromator (Oriel Cornerstone 130, Newport), and the signals were recorded on an oscilloscope (TDS 2022, Tektronix) communicated with a computer. Transmission electron microscopy (TEM) images were recorded on a Titan 80-300 TEM (FEI Co.) equipped with a monochromator, Cs probe-corrector, and Gatan image filter. The acceleration voltage of the TEM was 300 kV.

Sample preparations

All photophysical measurements were carried out in toluene using a 10 mm path quartz cuvette. The samples for UV-visible absorption measurements were prepared by purging with argon for at least 15 minutes. The samples for quantum yield and transient absorption measurements were prepared by at least 4 freeze-pump-thaw cycles.

The concentrations of CdS NCs were determined from absorption spectra using the molar extinction coefficient according to the empirical functions:[7]

$$D = (-6.6521 \times 10^{-8})\lambda^3 + (1.9557 \times 10^{-4})\lambda^2 - (9.2353 \times 10^{-2})\lambda + 13.29 \tag{1}$$

$$\varepsilon = 21536(D)^{2.3} \tag{2}$$

where λ is the excitonic peak in the UV-visible absorption spectra, D is the diameter of NCs and ε is the molar extinction coefficient at the excitonic peak.

The solid sample was prepared by soaking a piece of filter paper into the solution for UV-visible absorption measurement, letting all the solvent slowly evaporate at 60 °C in the dark.

Light sources

302 nm irradiation was performed using a UV analytic lamp ($\sim$10 mWcm^{-2} at the sample); 425 nm irradiation was carried out by using an Nd:YAG laser (10 ns, 10 Hz) equipped with an OPO set at 425 nm (2.0 mJ/pulse); 405 nm irradiation ($\sim$60 mWcm^{-2}) and 445 nm irradiation ($\sim$15 mWcm^{-2}) were carried out by using continuous-wave lasers (Coherent, OBIS) coupled with a concave lens; 590 nm irradiation ($\sim$15 mWcm^{-2} at the sample) was carried out using an LED light source (LED Engin, FWHM = 20 nm).

Quantum yield and conversion of photocyclization reactions

Photocyclization quantum yields were determined by using ferrioxalate actinometry according to standard methods.[8] Visible irradiation was carried out by using a continuous-wave laser (Coherent, OBIS) coupled with a neutral density (ND) filter to reduce the intensity. Fresh potassium ferrioxalate solutions (0.006 M, 3 ml) were irradiated for 1-5 min. 0.1 ml of the irradiated solution is mixed with 0.1 ml phenanthroline solution (0.1 wt%) and 0.05 ml of buffer solution (0.1 M NaOAc/0.18 M H_2SO_4) and subsequently diluted with water to 1 ml. The quantum flow of incident light was determined by ferrioxalete using equation 3:

$$I_0 = \frac{\Delta A_{510nm} V_1 V_3 N_L 10^{-3}}{\Delta t\, \Phi_{0\_irr}\, \varepsilon_{510nm}\, d V_2} \tag{3}$$

Where ΔA_{510nm} is the difference in absorbance at 510 nm, V_1 is the irradiated volume (3 ml), V_3 is the used volume for subsequent addition of phenanthroline buffer (0.1 ml), N_L is the Avogadro number, Δt is the irradiation time, Φ_{0_irr} is the quantum yield of ferrioxalate at the irradiated wavelength ($\Phi_{0\_405nm} = 1.14$), ε_{510nm} is the extinction coefficient of the complex ($\varepsilon_{510nm} = 1.11 \times 10^4\ Lmol^{-1}cm^{-1}$). d is the optical path length of the cuvette (1 cm), and V_2 is the volume used for UV-visible absorption measurements (1 ml).

To determine the quantum yields of the DAEs (Φ_{irr}) under visible light irradiation, mixed solutions (3 ml of 1 μM CdS NCs, 200 μM 3-PCA and 500 μM DAE-open) were prepared by at least 4 freeze-pump-thaw cycles, they were then irradiated with the same light sources (1-5 min) whose quantum flows have been determined by ferrioxalate. As the solutions did not completely absorb all the incident photons, the quantum flow of photons absorbed by the DAE samples (I) was calculated using equation 4:

$$I = I_0(1 - 10^{-A_{irr}}) \tag{4}$$

Where A_{irr} is the absorbance of the DAE mixtures at the irradiated wavelength.

The quantum yields of the DAEs under visible light irradiation was calculated using equation 5:

$$\Phi_{irr} = \frac{\Delta A_{closed\_peak} V_1 V_3 N_L 10^{-3}}{\Delta t\, I\, \varepsilon_{closed\_peak}\, d\, V_2} \tag{5}$$

Where ΔA_{closed_peak} is the difference in absorbance at the absorption peak of DAE-closed; V_1 is the irradiated volume (3 ml); $V_2 = V_3 = 3\ ml$, $\varepsilon_{closed\_peak}$ is the molar absorption coefficient of the peak maximum of DAE-closed.

The conversions of the DAEs under visible light irradiation were determined according to the UV-visible absorption spectra in Fig. 2b and 4a. The concentrations of DAE-open in the mixed solution are all 50 μM. The concentrations of DAE-closed were calculated using the molar absorption coefficient of the peak maximum in the visible band. The conversion from DAE1-open to DAE1-closed at the photostationary state (PSS) was reported as 94% upon 310 nm irradiation,[9] and the molar absorption coefficient of DAE1-closed was determined to be $\varepsilon_{530} = 1.94 \times 10^4\ M^{-1}cm^{-1}$ in toluene. The conversion of DAE2-open to DAE2-closed at the PSS was reported as 79% upon 313 nm irradiation[10], according to which the molar absorption coefficient of DAE2-closed in toluene was determined to be $\varepsilon_{575} = 1.25 \times 10^4\ M^{-1}cm^{-1}$. The corresponding conversions (α) at the PSS upon 405 nm light irradiation were calculated using equation 6.

$$\alpha = \frac{A_{closed\_peak}}{\varepsilon_{closed\_peak}\, d\, c_0} \tag{6}$$

where A_{closed_peak} is the absorbance of the band peak of DAE-closed at the PSS after visible light irradiation, i.e, $A_{530} = 0.91$ for DAE1-closed, $A_{575} = 0.36$ for DAE2-closed; $\varepsilon_{closed\_peak}$ is the molar absorption coefficient of DAE-closed at the peak absorption, i.e. $\varepsilon_{522} = 1.97 \times 10^4\ M^{-1}cm^{-1}$ for DAE1-closed, $1.25 \times 10^4\ M^{-1}cm^{-1}$ for DAE2-closed.; d is the optical path of the cuvette (1 cm); c_0 is the concentration of DAE-open in the mixed solution (50 μM).

Computational details

Density functional calculations (DFT) were performed using the Gaussian 16 software package[11] using the hybrid functional B3LYP and the basis set 6-311+G(d,p). Full optimization of the ground-state structure was followed by excited state calculations using the basis set 6-31G(d). Vertical excitation energies from the ground state equilibrated geometry (12 lowest of both triplet and singlet spin) were calculated using the time-dependent formalism (TDDFT).

2. TEM images, absorption and PL spectra of CdS NCs

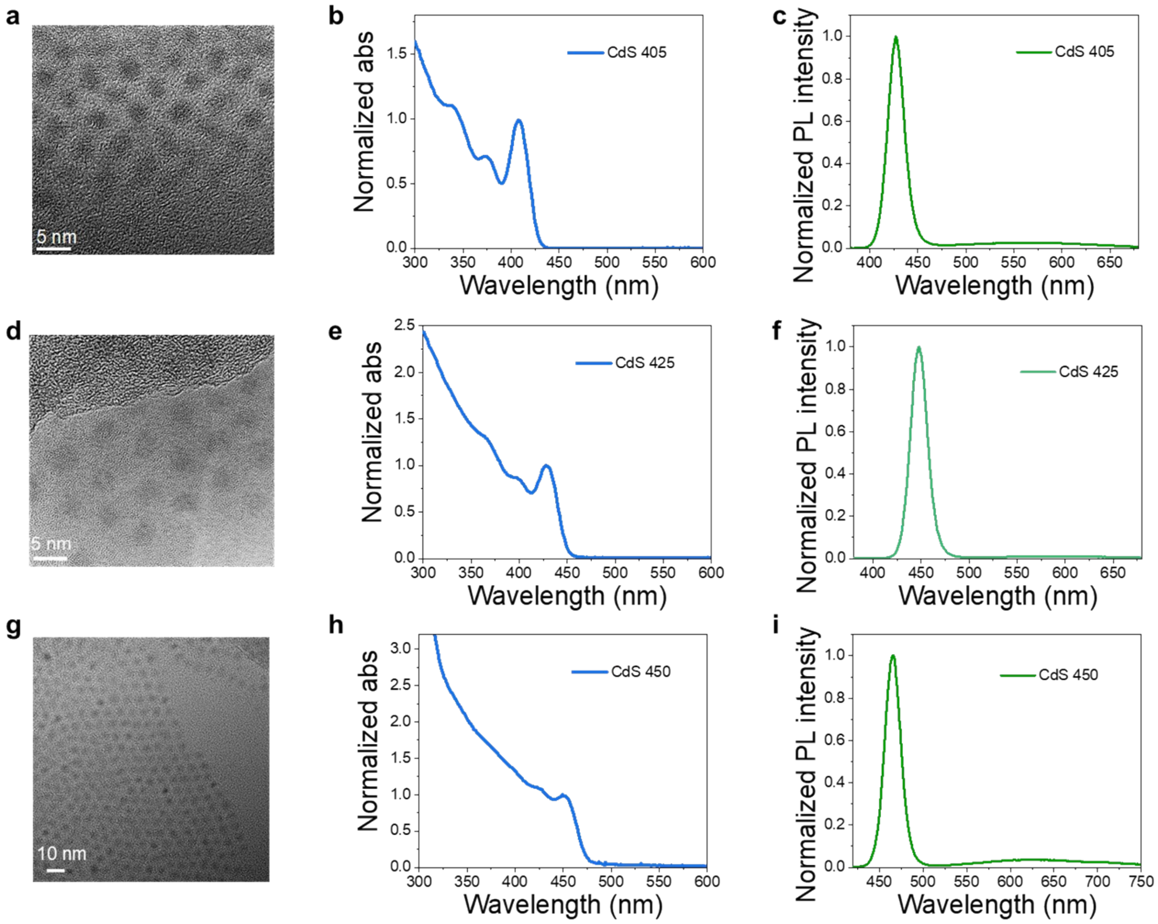

Fig. S1. Spectroscopy of CdS NCs. a. TEM image of CdS 405, **b.** Normalized UV-visible absorption of CdS 405 in toluene, **c.** PL spectrum of CdS 405 in toluene; **d.** TEM image of CdS 425, **e.** Normalized UV-visible absorption of CdS 425 in toluene, **f.** PL spectrum of CdS 425 in toluene, **g.** TEM image of CdS 450, **h.** Normalized UV-visible absorption of CdS 450 in toluene, and **i.** PL spectrum of CdS 450 in toluene.

3. Light response of DAE1

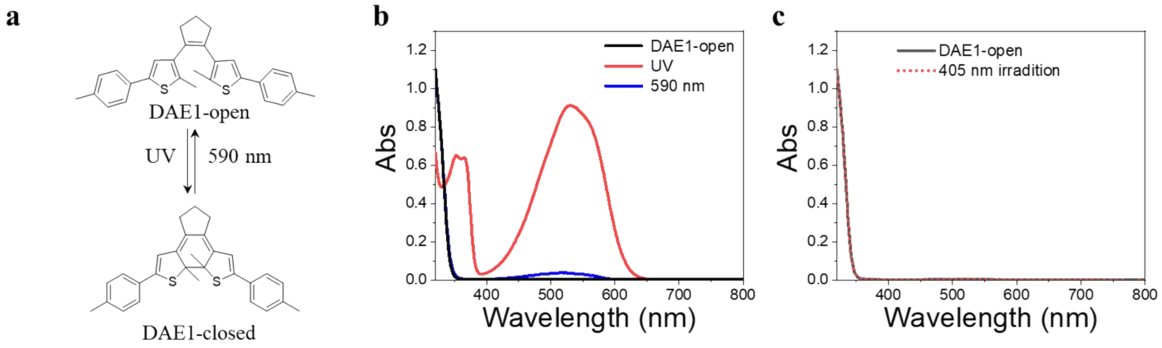

Fig. S2. **Light response of DAE1. a.** Photoisomerization of DAE1 under UV and 590 nm light irradiation. **b.** UV-visible absorption spectra of DAE1-open (50 µM) in toluene before (black-line) and after 302 nm (30 s, red-line), and then the same sample was irradiated at 590 nm (90 s, blue-line) after the exposure of UV irradiation. **c.** UV-visible absorption spectra of DAE1-open (50 µM) in toluene before and after 405 nm light irradiation (120 s).

4. PL quenching of CdS NCs by 3-PCA

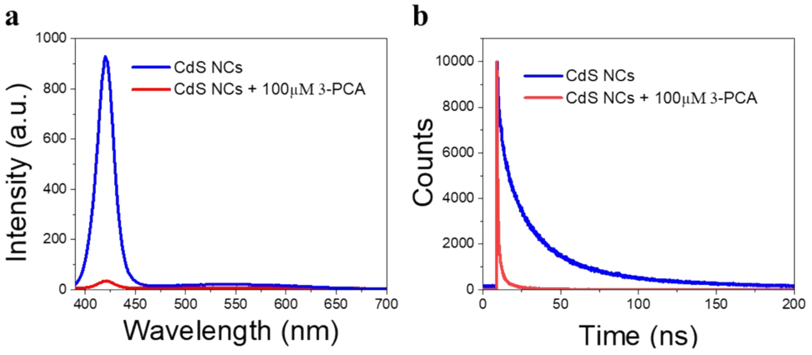

Fig. S3. PL quenching of CdS 405 by 3-PCA. a. PL spectra and **b.** time-resolved PL decay of CdS NCs (CdS 405) with and without the mediator 3-PCA (100 µM).

PL decay of CdS NCs exhibits complicated multiple exponential components. Herein three exponentials decay was used to achieve a satisfactory fit:

$$I = I_0 \sum_{i=1}^{3} A_i e^{-t/\tau_i} \tag{7}$$

where A_i and τ_i are the amplitude and lifetime of the i:th exponential component, respectively. The decays were deconvoluted using the instrument response function (IRF). The amplitude-weighted average lifetimes were calculated using equation 8

Amplitude-weighted: $$<\tau> = \frac{\sum_{i=1}^{3} A_i \tau_i}{\sum_{i=1}^{3} A_i} \tag{8}$$

The efficiency of the first triplet energy transfer (TET$_1$), Φ_{TET1}, was estimated from PL lifetime quenching using equation 9

$$\Phi_{TET1} = 1 - <\tau> / <\tau>_0 \tag{9}$$

where $<\tau>$ and $<\tau>_0$ are the amplitude-weighted average PL lifetimes of CdS NCs with and without the mediator, respectively.

The amplitude-weighted PL liftetime of CdS 405 is reduced from 16.0 ns to 1.5 ns after adding 3-PCA, and the TET$_1$ efficiency was calculated to be 91%, which was also consistent with the efficiency estimated from PL intensity quenching.

The number of bound 3-PCA molecules per NC of CdS 405 (m) can be estimated using a Poisson binding model[12] that can be applied to fit the PL decays in Fig. S3b:

$$PL(t) = PL_0(t) \times exp\left[- m(1 - e^{-k_q t})\right] \tag{10}$$

Here, $PL(t)$ and $PL_0(t)$ are the multi-exponential decays of CdS 405 with and without 3-PCA, respectively, and k_q is the quenching rate per bound ligand. Fitting PL decays of CdS 405 with 3-PCA in Fig. S3b using Equation 10 results in values for k_q of circa 0.2 ns^{-1} and $m = 21$.

5. DAE1 mixtures under visible light irradiation.

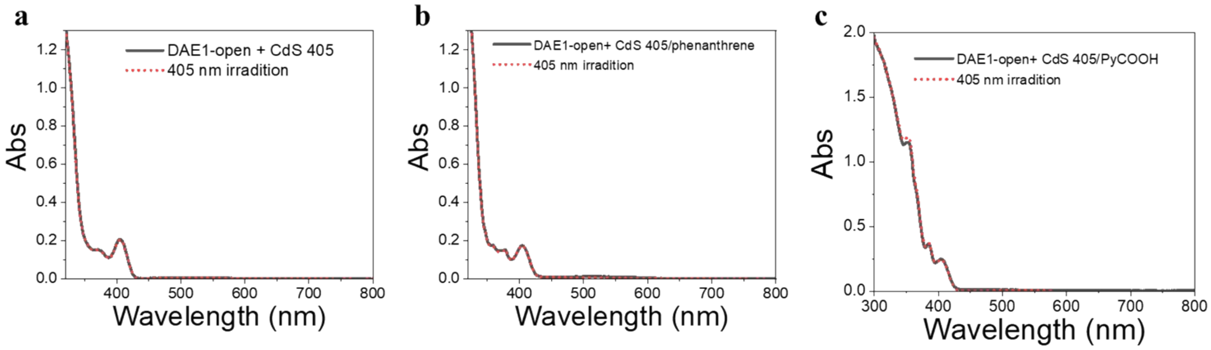

Fig. S4. Visible light response of DAE1 mixtures. a. UV-visible absorption spectra of DAE1 (50 μM) mixed with CdS 405 (0.5 μM) in deaerated toluene before (black-line) and after 405 nm visible light irradiation (120s, red-dot). **b.** UV-visible absorption spectra of DAE1 (50 μM) mixed with CdS 405 (0.5 μM) and phenanthrene (100 μM) in deaerated toluene before (black-line) and after 405 nm visible light irradiation (120 s, red-dot). **c.** UV-visible absorption spectra of DAE1 (50 μM) mixed with CdS 405 (0.5 μM) and PyCOOH (100 μM) in deaerated toluene before (black-line) and after 405 nm visible light irradiation (120 s, red-dot). In all the three cases, 405 nm light irradiation did not result in any obvious photoisomerization of DAE1.

6. PL quenching of CdS 405 by PyCOOH

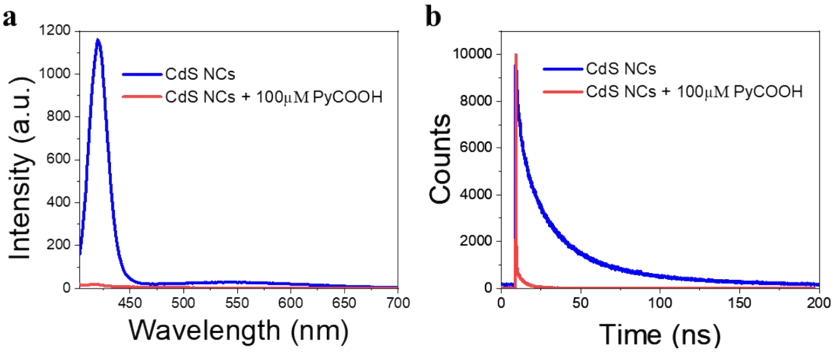

Fig. S5. PL quenching of CdS 405 by PyCOOH. a. PL spectra and **b.** time-resolved PL decay of CdS NCs (CdS 405, 0.5 μM) with and without the mediator PyCOOH (100 μM) in toluene.

The amplitude-weighted PL liftetime of CdS 405 is reduced from 16.0 ns to 1.9 ns after adding PyCOOH (100 μM), and the TET_1 efficiency was calculated to be 88% using equation 8, which was very similar to the efficiency estimated from PL intensity quenching.

7. Individual components for all-visible-light activated DAE2

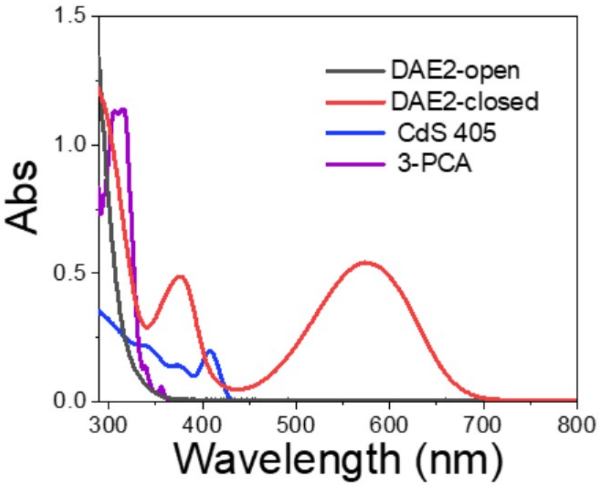

Fig. S6. UV-visible absorption spectra of the individual components. DAE2-open (50 μM, black), DAE2-closed converted from the open form under 313 nm UV light irradiation (red), CdS 405 (0.5 μM, blue) and 3-PCA (100 μM, purple) in toluene.

8. DAE3 and DAE4 under visible light irradiation

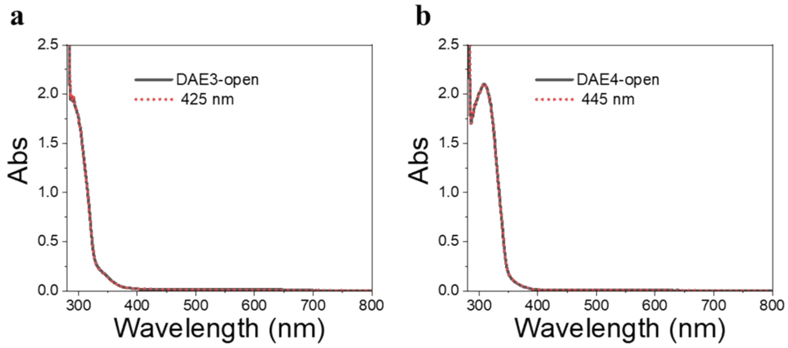

Fig. S7. Visible light response of DAE3 and DAE4. a. UV-visible absorption spectra of DAE3 (50 μM) in toluene before (black-line) and after 425 nm visible light irradiation (10 min, red-dot). **b.** UV-visible absorption spectra of DAE4 (50 μM) in toluene before (black-line) and after 445 nm visible light irradiation (9 min, red-dot). In these two cases, visible light irradiation did not result in any obvious photoisomerization of the DAEs.

9. DAE1 mixture under visible light irradiation in an air-equilibrated solution

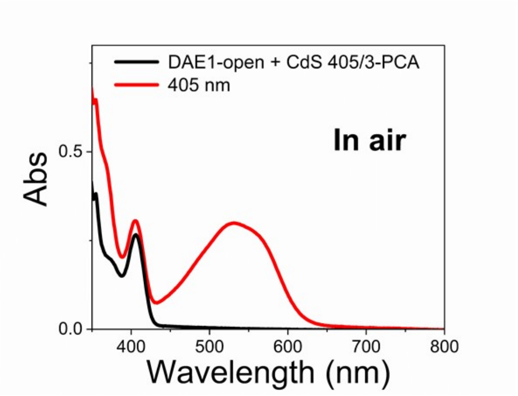

Fig. S8. Visible light response of DAE1 mixed with CdS 405 and 3-PCA in an air-equilibrated solution. UV-visible absorption spectra of DAE1-open (50 μM) mixed with CdS 405 and 3-PCA prepared in aerated toluene before (black) and after 405 nm light irradiation (120 s, red-line).

10. DFT calculations of the first excited triplet states of the DAEs

Table S1. Energy of the first excited triplet states (T_1) of the investigated DAEs from TDDFT calculations on optimized ground state geometries.

Structure	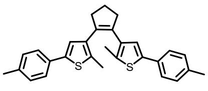 DAE1-open	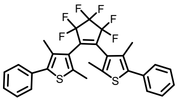 DAE2-open	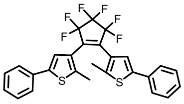 DAE3-open	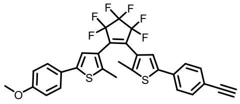 DAE4-open
T_1 (eV)	2.5 eV	2.8 eV	2.6 eV	2.5 eV

11. References

1. E. Orgiu, N. Crivillers, M. Herder, L. Grubert, M. Patzel, J. Frisch, E. Pavlica, D. T. Duong, G. Bratina, A. Salleo, N. Koch, S. Hecht and P. Samori, *Nat. Chem.*, 2012, **4**, 675-679.

2. P. A. Liddell, G. Kodis, A. L. Moore, T. A. Moore and D. Gust, *J. Am. Chem. Soc.*, 2002, **124**, 7668-7669.
3. S. Hermes, G. Dassa, G. Toso, A. Bianco, C. Bertarelli and G. Zerbi, *Tetrahedron Lett.*, 2009, **50**, 1614-1617.
4. L. Hou, A. Olesund, S. Thurakkal, X. Zhang and B. Albinsson, *Adv. Funct. Mater.*, 2021, **31**, 2106198.
5. W. W. Yu and X. G. Peng, *Angew. Chem. Int. Ed.*, 2002, **41**, 2368-2371.
6. Z. Li, Y. J. Ji, R. G. Xie, S. Y. Grisham and X. G. Peng, *J. Am. Chem. Soc.*, 2011, **133**, 17248-17256.
7. W. W. Yu, L. H. Qu, W. Z. Guo and X. G. Peng, *Chem Mater*, 2003, **15**, 2854-2860.
8. M. Montalti and S. L. Murov, *Handbook of photochemistry*, CRC/Taylor & Francis, Boca Raton, 3rd edn., 2006.
9. M. Herder, B. M. Schmidt, L. Grubert, M. Patzel, J. Schwarz and S. Hecht, *J. Am. Chem. Soc.*, 2015, **137**, 2738-2747.
10. M. Irie, K. Sakemura, M. Okinaka and K. Uchida, *J. Org. Chem.*, 1995, **60**, 8305-8309.
11. M. J. Frisch, G. W. Trucks, H. B. Schlegel, G. E. Scuseria, M. A. Robb, J. R. Cheeseman, G. Scalmani, V. Barone, G. A. Petersson, H. Nakatsuji, X. Li and M. Caricato, Gaussian 16, Reversion C. 01e, 2016.
12. G. B. Piland, Z. Y. Huang, M. L. Tang and C. J. Bardeen, *J. Phys. Chem. C*, 2016, **120**, 5883-5889.